Boundary effect on specific fracture energy of concrete

K. Duan* & X.Z. Hu
School of Mechanical Engineering, University of Western Australia, 35 Stirling Highway, Crawley, WA 6009, Australia

F.H. Wittmann
Qingdao Institute of Architecture and Engineering, Centre for Durability, Maintenance, and Repair, Qingdao, P.R. China

**Email: kaiduan@mech.uwa.edu.au, Fax: 61-8-9380-1024*

ABSTRACT: The influence of specimen back-face boundary on the shape and size of the crack-tip fracture process zone during crack growth is related to the fracture energy distribution along the crack path. The governing mechanism responsible for the size effect on the specific fracture energy of concrete is the height variation of the crack-tip fracture process zone. Such a height variation exists in the boundary zone where the development of the crack-tip fracture process zone is limited due to the confined space and sharp stress gradient. The reduction in the fracture process zone height leads to a decreasing specific fracture energy distribution along the crack path in the back-face boundary region. The adhesive thickness effect on the critical energy release rate of the adhesive joint sandwiched between two non-yielding substrates and the un-cracked ligament effect on the large scale yielding of polymers and metals provide further proof to the relationship between the height variation of the crack-tip plastic zone and the specific fracture energy.

Keywords: boundary effect, size effect, fracture energy, fracture process zone (FPZ), FPZ height

1 INTRODUCTION

The size effect on the specific fracture energy G_f defined by RILEM (1985) and on the nominal tensile strength of concrete is an important part of fracture mechanics of concrete and concrete structures. The size effect on the nominal tensile strength of concrete is dealt with specifically in a separate contribution to the conference (Duan & Hu 2004). Therefore, the main focus of the present paper is on the specific fracture energy G_f and its associated size effect.

In our previous work, we have introduced a local fracture energy concept to explain the size effect on the RILEM defined G_f (Hu 1990, Hu & Wittmann 1992). Recently, the same concept has also been adopted by others (Abdalla & Karihaloo 2003) and confirmed by their experimental results. In our recent work, we have simplified the previous local fracture energy distribution using a bilinear function to approximate the local fracture energy distribution (Duan et al 2001, 2002, 2003c,d). This bilinear simplification is necessary because of the introduction of the inner zone and boundary zone concept.

It is known that the RILEM defined specific fracture energy G_f is averaged over the entire fracture area, which is the same as assuming a constant fracture energy distribution. The size effect on the RILEM defined G_f exists, simply because the imbedded assumption of a constant fracture energy distribution is too rough. The local fracture energy g_f concept refines the RILEM definition by separating the total fracture area into two different regions: the inner zone and boundary zone. Within the inner zone, a constant fracture energy distribution (g_f = G_F = constant) exists, which is similar to the RILEM G_f definition, except it only covers the inner zone of a specimen. In the boundary zone, the local fracture energy g_f decreases linearly from G_F to g_0 (≈ 0 for concrete and mortar), the essential work of fracture, corresponding to the case without the crack-tip fracture process zone (FPZ), or zero FPZ height.

In this paper, we are going to show the variation of the FPZ height, h_{FPZ}, controls the size effect on the specific fracture energy G_f defined by RILEM. Similarly, the crack-tip plastic zone height (also denoted by h_{FPZ} for simplicity) controls the adhesive thickness effect on the critical strain energy release rate of the adhesive joint sandwiched between two non-yielding substrates. The well-established essential work of fracture (EWF) model (Cotterell & Reddell 1977, Mai & Cotterell 1980,

Atkins & Mai 1985) for large scale yielding of polymers and metals provides another convincing support to the concept, i.e. the boundary influence leads to the variation of the crack-tip plastic zone height, which then leads to the common size effect.

2 MODELLING OF BOUNDARY EFFECT

2.1 *Local fracture energy model*

The specific fracture energy G_f defined by RILEM is given by:

$$G_f = \frac{1}{B \cdot (W-a)} \cdot \int P \cdot d\delta \qquad (1)$$

in which B is the specimen thickness, a is the crack length, and W is the specimen width. The total fracture energy, $\int P \cdot d\delta$, determined by the complete load and load-point-displacement (P-δ) curve is averaged over the entire fracture area measured by $B \cdot (W-a)$. The RILEM G_f is illustrated in Figure 1(a) by the dash line, i.e. a constant fracture energy distribution over the crack path (W-a) is assumed. In other word, RILEM has assumed a constant "local fracture energy" distribution.

The concept of the local fracture energy (Hu 1990, Hu & Wittmann 1992) believes The RILEM G_f definition Equation 1 is too rough, as it has virtually assumed the crack-tip FPZ, in which the fracture energy dissipation occurs, could remain constant during the entire crack growth process. The specific fracture energy should be related to the localized fracture energy dissipation and then the corresponding FPZ. Therefore, the local specific fracture energy g_f was introduced, $g_f = g_f(x)$, where $0 \le x \le (W-a)$. According to the energy conservation principle, it can be established that:

$$G_f = \frac{1}{(W-a)} \cdot \int_0^{W-a} g_f \cdot dx \qquad (2)$$

For a fixed specimen size W, the RILEM G_f often varies with the initial crack length a (Hu & Wittmann 1992). As a result, the relationship $G_f = G_f(a)$ can be measured in experiments for $0 < a < W$. The $G_f(a)$ function can then be used to determine the local fracture energy distribution $g_f(a)$ as a function of the position parameter a (Hu 1990, Hu & Wittmann 1992), i.e.

$$g_f = G_f(a) - (W-a) \cdot \frac{dG_f(a)}{da} \qquad (3)$$

Therefore, the local fracture energy g_f distribution is well defined using the RILEM G_f measurements, and no assumption is required for the g_f distribution.

The recent work (Duan et al 2001, 2002, 2003c,d) has found that even a simple bi-linear function can capture the major boundary influence on the RILEM G_f. As illustrated in Figure 1(b), the FPZ size or height h_{FPZ} remains constant in the inner zone away from the specimen back-face boundary, and so does the local fracture energy g_f as shown in Figure 1(a). In the boundary zone illustrated in Figure 1(b), the FPZ size or height h_{FPZ} decreases because of the decreasing un-cracked ligament and sharp stress gradient in the boundary zone. As a result, the local fracture energy g_f also decreases as shown in Figure 1(a). g_0 is the essential work of fracture for $h_{FPZ} = 0$. As a first approximation, a linear distribution has been assumed for g_f in the boundary zone.

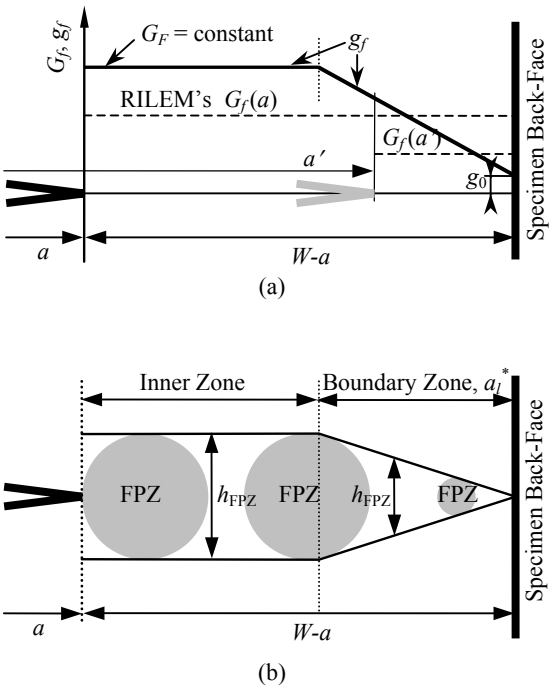

Figure 1. Separation of inner and boundary zones by a_l^* in a specimen of width W and crack a. (a) Corresponding bi-linear local energy g_f distribution in comparison with the RILEM G_f as the average fracture energy. (b) Variation of FPZ and its height h_{FPZ} in the inner and boundary zones.

Figure 1(a) illustrates two different situations: the crack a in the inner zone, and the crack a' in the boundary zone. The RILEM $G_f(a) > G_f(a')$ because $G_f(a')$ is only associated with much smaller FPZ

confined in the boundary zone. Clearly, if the inner zone is dominant, as in the case of a very large specimen, $G_f(a) = G_F$.

The inner and boundary zones are separated by the reference crack a_l^*, as illustrated in Figure 1(b). Substituting the bi-linear function of the local fracture energy g_f as shown in Figure 1(a) into Equation 2, it can be found that:

$$G_f = \begin{cases} G_F - \dfrac{a_l^*}{2(W-a)} \cdot (G_F - g_0), & W - a \geq a_l^* \quad \text{(a)} \\ g_0 + \dfrac{(W-a)}{2a_l^*} \cdot (G_F - g_0), & W - a \leq a_l^* \quad \text{(b)} \end{cases} \tag{4}$$

The size independent fracture energy G_F and the essential work of fracture g_0 are material properties. The reference crack a_l^*, will change with the specimen geometry and loading condition, which determine the stress field and then the FPZ and h_{FPZ}. For concrete and mortar, the essential work of fracture g_0 is close to zero and hence can be neglected (Hu 1990, Hu & Wittmann 1992, Duan et al 2003c,d). Therefore, if $g_0 \approx 0$, Equation 4 only contains two unknown parameters: G_F the material constant, and the reference crack a_l^* or the geometry and loading condition parameter.

In general, $G_F \geq G_f \geq g_0$, and G_F and g_0 actually become the two asymptotic limits of the RILEM defined G_f for very large and very small specimens.

2.2 *"Essential work of fracture" model*

The EWF model was developed to study the behavior of the specific fracture energy G_f associated with the large scale yield failure of ductile polymers and metals (Cotterell & Reddell 1977, Mai & Cotterell 1980, Atkins & Mai 1985). The G_f definition used by EWF is the same as that of RILEM specified by Equation 1. Although the types of failure and materials dealt with by EWF cannot be more different to concrete and the associated quasi-brittle fracture behavior, EWF is in fact consistent with the boundary effect model outlined in Section 2.1.

The typical specimen geometry used by EWF is illustrated in Figure 2(a), a double-edge notched specimen with two deep notches so that full yielding precedes material fracture initiation. A single edge notched specimen shown in Figure 2(b) can also be used by EWF if the un-notched ligament area $B\cdot(W\text{-}a)$ is small. Comparing Figures 1(b) and 2(b), it is clear that EWF actually models the influence of the specimen back-face boundary on the specific fracture energy G_f, which should be similar to Equation 4(b) for very short ligament.

EWF assumes that G_f can be separated into two different energy measurements: the essential work of fracture g_0 corresponding to zero plastic zone height ($h_{FPZ} = 0$), and the plastic work g_p per unit projected area. The total plastic work is determined by the volume of the crack-tip plastic zone V_p times the plastic work density ρ_p, which is assumed to be a material constant. Therefore,

$$\begin{aligned} G_f &= g_0 + g_p \\ &= g_0 + \frac{\rho_p \cdot V_p}{B \cdot (W-a)} \end{aligned} \tag{5}$$

Let us still use h_{FPZ} to represent the crack-tip plastic zone height. In general, V_p = constant$\cdot B(W\text{-}a)\cdot h_{FPZ}$. For the circular shape assumed by EWF, the "constant" = $\pi/4$, and $h_{FPZ} = W\text{-}a$. Therefore, Equation 5 can be rewritten as follows:

$$\begin{aligned} G_f &= g_0 + \frac{\rho_p \cdot \text{constant} \cdot B \cdot (W-a) \cdot h_{FPZ}}{B \cdot (W-a)} \\ &= g_0 + C_\rho \cdot h_{FPZ} = g_0 + C_\rho \cdot (W-a) \end{aligned} \tag{6}$$

where C_ρ is constant. It is clear that although EWF deals with the ligament effect on G_f, it actually models the influence of the plastic zone height h_{FPZ} on the specific fracture energy.

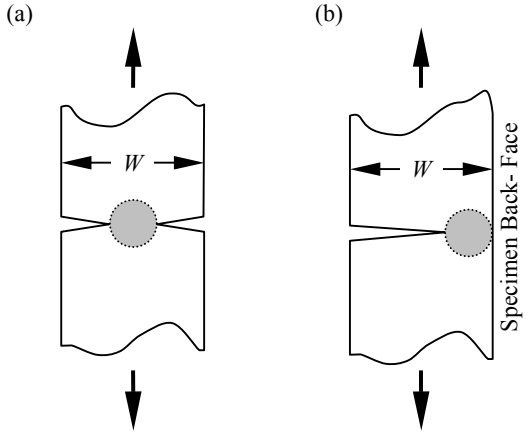

Figure 2. (a) Common EWF specimen showing the influence of deep double notches on the plastic zone and then G_f, and (b) deep single notched EWF specimen showing the influence of specimen back-face on the plastic zone and then G_f.

Since Equation 6 models the specimen back-face influence as indicated in Figure 2(b), EFW provides a direct support of the boundary effect model summarized in Section 2.1. In fact, within the boundary zone shown in Figure 1(b), the boundary effect model, Equation 4(b), and EWF, Equation 6, are identical.

It can be easily proven from Equation 3 that a linear G_f function is defined by a linear local fracture energy g_f function. Therefore, the suitability of the bi-linear g_f distribution illustrated in Figure 1(a) is justified by the combination of the constant G_f distribution assumed by RILEM, and the linear G_f modeling result from EWF in the boundary region.

2.3 *Modeling of adhesive thickness effect*

The adhesive and non-yielding metal substrate system shown in Figure 3 offers the most direct evidence on the influence of the plastic zone height h_{FPZ} on the specific fracture energy G_f because the adhesive thickness is identical to h_{FPZ}.

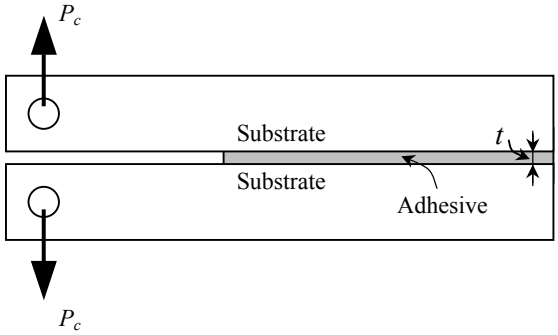

Figure 3. Common DCB specimen used to measure the critical strain energy release rate G_C of adhesive joint. The adhesive/substrate system is linear elastic up to the critical load P_C. The initial crack is long so that $G_C = G_f$.

The critical strain energy release rate G_C is commonly used to characterize the fracture toughness of the adhesive joint. For the double-cantilever-beam (DCB) geometry, the typical load and load-point displacement curve remains linear up to the maximum load at which unstable fracture occurs. The initial crack of the DCB specimen is long enough so that $G_C = G_f$ at the unstable fracture point, and the maximum plastic zone can be fully developed for the given adhesive thickness t.

It has been recently proven (Duan et al 2003a,b) that the critical strain energy release rate G_C (or the specific fracture energy G_f) is given by:

$$G_C = G_f = \begin{cases} g_0 + \dfrac{(G_{\max} - g_0)}{t_{\max}} \cdot t \ , & t < t_{\max} \\ G_b + (G_{\max} - G_b) \cdot \left(\dfrac{t}{t_{\max}} \right)^{-C \cdot \left(\frac{G_{\max}}{t_{\max}} \right)} , & t > t_{\max} \end{cases} \quad (7)$$

The essential work of fracture g_0 and G_b are the material properties of the bulk adhesive. The scaling constant C is 7.32 for t in mm, and G_{max} in kJ/m^2, which is determined and confirmed by experimental results of different sources (Duan et al 2003a,b). The two remaining parameters G_{max} and t_{max} represent the optimum adhesive joint properties. The initial slope, G_{max}/t_{max}, is related to the substrate modulus, and the constraint factor defined by the t^*_B/t_B ratio (Duan et al 2003a,b). The thickness or plastic zone height measurements, t^*_B and t_B, have been illustrated in Figure 4 together with the $G_C - t$ (or G_C - h_{FPZ}) relationship for the adhesive joint.

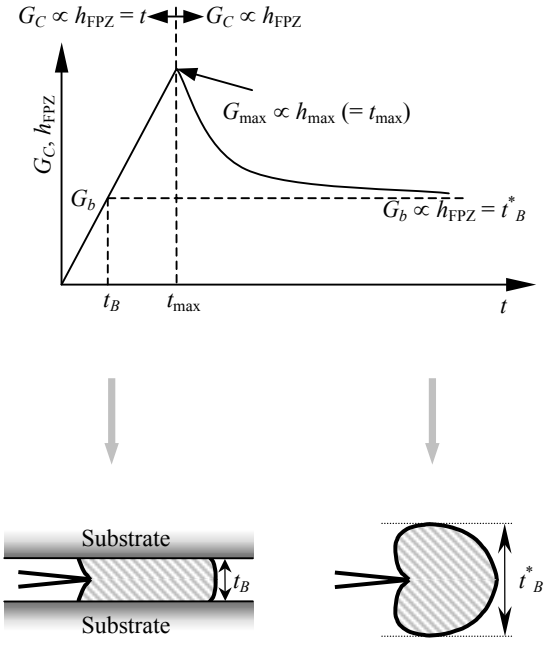

Figure 4. Simplified $G_C - t$ (or G_C - h_{FPZ}) relationship for adhesive joint. The plastic zone height t^*_B is related to G_b for the bulk adhesive, t_B is related to $G_C = G_b$ for the adhesive joint. The initial slope G_{max}/t_{max} is then related to the constraint factor t^*_B/t_B (Duan et al 2003a,b).

G_b in Equation 7 represents the critical strain energy release rate of the bulk adhesive. The maximum critical strain energy release rate G_{max} of the adhesive joint is actually higher than G_b because the maximum plastic zone height of the adhesive joint t_{max} exceeds the height of a fully developed plastic zone t^*_B in the bulk adhesive due to the constraint effect from the non-yielding substrates.

Equation 7 for $t < t_{max}$ (then $t = h_{FPZ}$) is identical with Equations 6 and 4(b). Although three very different material systems are studied here, the same linear relationship between G_f - h_{FPZ} has been established, indicating the variation in h_{FPZ} is the dominant mechanism responsible for the size effect on concrete fracture, ligament effect on polymer and metal fracture, and thickness effect on adhesive joint fracture.

Since the variation in h_{FPZ} occurs in the specimen boundary region (in bulk concrete, polymer and metal samples) or varies with the bi-material interfacial boundaries (adhesive joint), the terminology of "boundary effect" is more adequate than "size effect".

3 ANALYSIS OF EXPERIMENTAL RESULTS

3.1 *Size and ligament effect on G_f of concrete*

The concrete results of three-point-bend (3-p-b) specimens with a span-to-depth (S/W) ratio of 6 (Nallathambi et al 1984) are selected to work out the size independent specific fracture energy G_F and the essential work of fracture g_0 using the boundary effect model, Equation 4. Here, G_F and g_0 are two material constants, one corresponding to the fully developed FPZ (maximum possible h_{FPZ}) and the other corresponding to zero FPZ ($h_{FPZ} = 0$).

Specimens of different α-ratios ($\alpha = a/W$) and W of 140, 200, 240 and 300 mm were tested, and the results are shown in Figure 5, showing clear specimen size and α-ratio effects.

The experimental results can be analyzed in two different ways. First, the four sets of data can be used together to work out the material constant G_F and g_0, and the results are shown in Table 1. Second, G_F and g_0 can be estimated using a single set of data with a fixed specimen size W, and the results are shown in Table 2. The averaged G_F and g_0 from the four sets of data are 134.2 and 5.66 N/m. Therefore, both methods give the identical G_F and a very small g_0. Clearly, the essential work of fracture g_0 corresponding to zero FPZ can be taken as zero without introducing any error on G_F (Duan et al 2002, 2003c).

Table 1: G_F and g_0 from four sets of data together

W (mm)	140	200	240	300
g_0 (N/m)	4.53	4.53	4.53	4.53
G_F (N/m)	134.1	134.1	134.1	134.1
a_l^* (mm)	81.92	105.1	117.6	144.7
a_l^*/W	0.585	0.526	0.490	0.482

Table 2: G_F and g_0 from one set of data with constant size W

W (mm)	140	200	240	300
g_0 (N/m)	8.29	0	7.36	7.00
G_F (N/m)	131.3	139.6	135.6	130.1
a_l^* (mm)	82.66	106.7	122.4	141.2
a_l^*/W	0.590	0.533	0.510	0.471

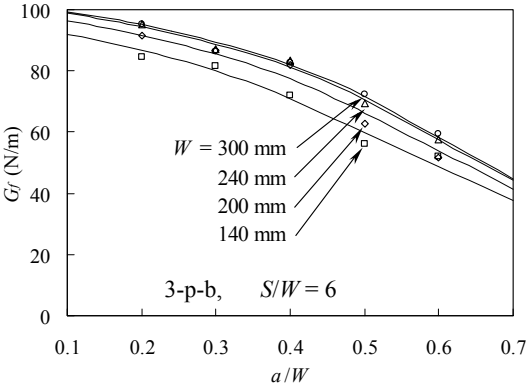

Figure 5. Size and α-ratio effects on G_f of concrete (Nallathambi et al 1984). The span and depth (S/W) ratio was fixed at 0.6.

Taking G_F = 134.1 N/m from Table 1 as the accurate answer, the relative errors from Table 2 are in the range of –3 % to 4 %. This is an excellent result, as it proves the material constant G_F can be accurately determined from specimens of a given size W, but different α-ratios. Clearly, the α-ratio or ligament dependence of the RILEM defined G_f is the same as the size effect observed from geometrically similar specimens.

3.2 *Ligament effect on G_f of mortar*

The mortar results from Hu and Wittmann (1992) are analyzed again to affirm the pertinence of the bi-linear distribution of the local fracture energy g_f, and to estimate the size independent G_F and the essential work of fracture g_0 of the material.

The wedge-splitting specimen geometry with size W = 180 mm was used, and the results are shown in Figure 6. In the previous study (Hu 1990, Hu & Wittmann 1992), the reference crack a_l^* was

assumed to corresponding to α = 0.7, or a_l^*/W = 0.3, which gave G_F = 43.9 N/m, and g_0 = 9.2 N/m.

Equation 4 can be used to determine G_F, g_0 and a_l^* from the results in Figure 6, or to determine G_F and g_0 with the assumed ratio of a_l^*/W = 0.3 following the previous work (Hu 1990, Hu & Wittmann 1992). Both curves are also plotted in Figure 6. The results are: G_F = 45.7 N/m and g_0 = 0.0 N/m with a_l^*/W = 0.256 from the results in Figure 6, and G_F = 46.3 N/m and g_0 = 5.3 N/m with the presumed a_l^*/W = 0.3. Clearly, the size independent G_F results are almost identical.

For comparison, the two local fracture energy g_f distributions, based on bi-linear and exponential function respectively, from the previous work are shown in Figure 7 (Hu 1990, Hu & Wittmann 1992). A Weibull-like distribution function was used to fit the experimental results of the RILEM G_f. Equation 3 was then used to work out the exponential g_f distribution. Interestingly, a linear function was obtained even from the exponential distribution within the specimen back-face boundary zone.

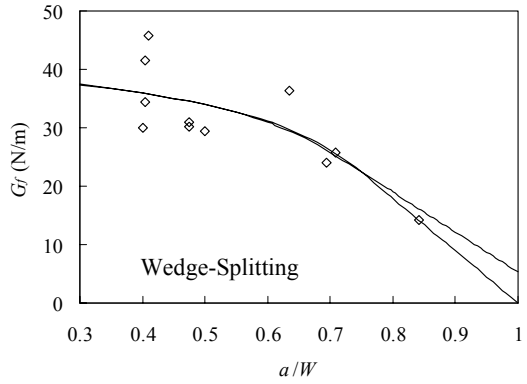

Figure 6. Ligament effect on G_f of mortar (Hu 1990, Hu & Wittmann 1992). Equation 4 gives G_F = 45.71 N/m, g_0 = 0.03 N/m and a_l^* = 46.06 mm, or G_F = 46.3 N/m and g_0 = 5.3 N/m with the presumed a_l^* = 54 mm.

g_0 = 9.2 and 7.1 N/m for the bi-linear and exponential function, respectively. In all cases discussed in this section, a small essential work of fracture is estimated, which is also consistent with the concrete results in Section 3.1.

3.3 *Thickness effect on G_C of Adhesive joint*

The adhesive joint model, Equation 7, is used to provide a further confirmation on the relationship between G_C (= G_f) and h_{FPZ}. The results of a rubber-modified epoxy adhesive sandwiched between two mild steel substrates from Kinloch and Shaw (1981) are selected, which were obtained using the contoured DCB adhesive joint specimens. The elastic modulus of steel is around 207 GPa in comparison with a normal epoxy of around 2.4 GPa.

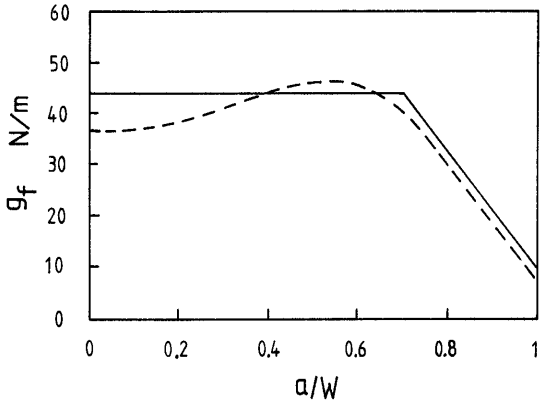

Figure 7. Local fracture energy g_f distributions estimated from the mortar resutls in Figure 6 (Hu 1990, Hu & Wittmann 1992). Both distributions defined similar G_F and g_0, and predicted almost identical linear g_f function in the specimen back-face boundary region.

Figure 8a,b shows the critical strain energy release rate G_C with specimen thickness of 50 and 3 mm, respectively. Equation 7 is applied to the experimental results in Figure 8(a) (Duan et al 2003a), with the pre-determined bulk adhesive property, g_0 = 0 and 0.5 kJ/m^2 (thin and thick lines, respectively). The corresponding maximum plastic zone height t_{max} = h_{FPZ} = 0.887 and 0.893 mm, and G_b = 1.39 and 1.40 kJ/m^2 respectively. Therefore, t_{max} = 0.89 mm and G_b = 1.40 kJ/m^2 are used. The scaling constant C = 7.32 for $t > t_{max}$ (G_{max} in kJ/m^2 and t_{max} in mm).

The same values of C, g_0 and t_{max} are used for the results in Figure 8(b) with specimen thickness of 3 mm. It is obtained that G_{max} = 2.3 kJ/m^2 and G_b = 1.65 kJ/m^2. The change in G_b represents the transition from the plane strain to plane stress condition. However, in both cases, the linear relationship between G_C (= G_f) and h_{FPZ} (= t) is confirmed for $t < t_{max}$. This is probably the most direct proof that the crack-tip plastic zone height or FPZ height (for quasi-brittle materials like concrete, and coarse-grained ceramics) is responsible for the change in the specific fracture energy G_f.

Similar linear relations between G_f and ligament length (= h_{FPZ}) have been found for bulk polymers and metals (Cotterell & Reddell 1977, Mai & Cotterell 1980, Atkins & Mai 1985). Therefore, the same linear relationship between G_f and h_{FPZ} is

confirmed for all the material systems considered in this study.

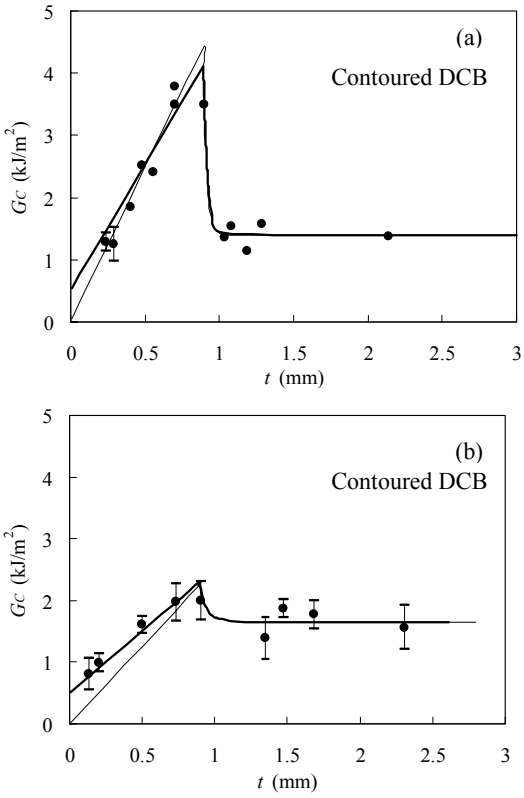

Figure 8. The thickness effects on the fracture energy GC of a rubber-modified epoxy adhesive sandwiched between two mild steel substrates (Kinloch & Shaw 1981) and the predictions using Equation 7. (a) B = 50 mm, g_0 = 0 & 0.5 kJ/m^2, t_{max} = 0.887 & 0.893 mm, G_{bulk} = 1.39 & 1.40 kJ/m^2, G_{max} = 4.41 & 4.11 kJ/m^2. Therefore, t_{max} = 0.89 mm and G_{bulk} = 1.40 kJ/m^2 are used. (b) B = 3 mm, G_{bulk} = 1.65 kJ/m^2, G_{max} = 2.3 kJ/m^2.

4 DISCUSSION AND CONCLUSIONS

The important roles of two specific fracture energy measurements, G_F and g_0, have been defined. G_F is related only to the maximum possible fully developed FPZ in a large specimen, and g_0 corresponds to the situation of zero FPZ. Therefore, both G_F and g_0 are material constants, and they represent two extreme limits.

The specific fracture energy G_f defined by RILEM is only an average measurement of the specific fracture energy distribution over the entire crack area. In general, $G_F \geq G_f \geq g_0$, which has G_F as the asymptotic limit of G_f for a very large specimen, and g_0 as the asymptotic limit of G_f for a very small specimen.

Since averaged over the entire fracture area, the RILEM G_f always contains the influence of the inner zone with a constant fracture energy distribution ($g_f = G_F$), and the influence of the boundary zone (g_f decreases linearly from G_F to g_0). If the inner zone is so dominant that the boundary zone can be neglected, $G_f = G_F$ and there is no size or ligament effect. If the inner and boundary zones are comparable, the ligament or size effect is obvious. Therefore, the size or ligament effect on the RILEM G_f reflects the influence of the boundary zone contribution. The two cracks, a and a', and the two RILEM fracture energy measurements, $G_f(a)$ and $G_f(a')$, shown in Figure 1(a) illustrate the boundary effect.

The common characteristic of the three models discussed in Section 2 is that the height of a crack-tip FPZ or plastic zone h_{FPZ} has been directly related to the local fracture energy g_f, and then the specific fracture energy G_f. The variation in h_{FPZ} leads to the variation in g_f, and then in G_f. The variation in h_{FPZ} during crack growth requires and defines the separation of the inner and boundary zones.

Three very different material systems are modeled, which include heterogeneous and quasi-brittle concrete, homogenous and ductile polymers and metals, and thin adhesive layer sandwiched between two hard and non-yielding substrates. However, the same linear dependence of G_f on h_{FPZ} has been identified, which supports the linear local fracture energy g_f assumption adopted for the specimen back face boundary region. Numerically, the same linear g_f distribution was also confirmed by Equation 3 using an exponential G_f function, as shown in Figure 7.

Clearly, the bi-linear g_f distribution is the simplest compromise, which is consistent with the RILEM defined constant fracture energy distribution in the inner zone, and consistent with EWF's linear fracture energy distribution in the specimen back-face boundary zone. The local fracture energy g_f concept allows the determination of the size independent G_F using relatively small specimens as long as a limited inner zone exists.

The four sets of concrete specimens of different sizes and α-ratios analyzed in Section 3.1 determine the same G_F value, which is probably the most convincing result to our best knowledge.

It is also found that the essential work of fracture g_0 is very small for concrete and mortar, and thus can be assumed as zero without introducing

any error in the size independent fracture energy G_F (Duan et al 2002, 2003c,d).

5 ACKNOWLEDGEMENTS

The financial support from the Australian Research Council (ARC) under the scheme of Discovery Grant is acknowledged.

REFERENCES

Abdalla, H.M. & Karihaloo, B.L. 2003. Determination of size-independent specific fracture energy of concrete from three-point bend and wedge splitting test. *Magazine of Concrete Research* 55(2): 133-141.

Atkins, A.G. & Mai, Y.W. 1985. Elastic and Plastic Fracture: Metals, Polymers, Ceramics, Composites, Biological Materials. Ellis Horwood Ltd., Chichester.

Cotterell, B. & Reddell, J.K. 1977. The essential work of plane stress ductile fracture. *International Journal of Fracture* 13: 267-277.

Duan, K. & Hu, X.Z. 2004. Asymptotic Analysis of Boundary-Effect on Strength of Concrete. This *proceeding*.

Duan, K., Hu, X.Z. & Mai, Y.W., 2003a. Substrate constraint and adhesive thickness effects on fracture toughness of adhesive joints. Accepted by *Journal of Adhesive Science and Technology*.

Duan, K., Hu, X.Z. & Mai, Y.W. 2003b. Modelling of thickness effect on fracture toughness of adhesive joints. To be presented to International Symposium on Macro-, Meso-, Micro- and Nano-Mechanics of Materials (MM2003), 8-10 December 2003HKUST, Clear Water Bay, Hong Kong.

Duan, K., Hu, X.Z. & Wittmann, F.H. 2001. Boundary effect on concrete fracture induced by non-constant fracture energy distribution. In R. de Borst, J. Mazars, G. Pijaudier-Cabot, J. G. M. van Mier (Eds.), *Fracture Mechanics of Concrete Structures (Proc. FraMCoS-4),* A.A.Balkema Publishers, Lisse, The Netherlands, Vol.1, pp.49-55.

Duan, K., Hu, X.Z. & Wittmann, F.H. 2002. Explanation of size effect in concrete fracture using non-uniform energy distribution. *Materials and Structures* 35, 326-331.

Duan, K., Hu, X.Z.& Wittmann, F.H. 2003c. Boundary Effect on Concrete Fracture and Non-Constant Fracture Energy Distribution. *Engineering Fracture Mechanics* 70: 2257-2268.

Duan, K., Hu, X.Z. & Wittmann, F.H. 2003d. Thickness Effect on Fracture Energy of Cementitious Materials. *Cement and Concrete Research* 33(4): 499-507.

Hu, X. Z. 1990. Fracture Process Zone and Strain Softening in Cementitious Materials. ETH Building Materials Reports No.1, ETH Switzerland. (AEDIFICATIO Publishers, 1995).

Hu X.Z, Wittmann F.H., 1992. Fracture energy and fracture process zone. Mater. Struct. 25, 319-26.

Kinloch, A.J. & Shaw, S.J. 1981. The Fracture Resistance of a Toughened Epoxy Adhesive Bond. *Journal of Adhesion* 12: 59-77.

Mai, Y.W. & Cotterell, B. 1980. Effect of pre-strain on plane stress ductile fracture in a-brass. *Journal of Material Science* 15: 2296-2306.

Nallathambi, P., Karihaloo, B.L. & Heaton, B.S. 1984. Effect of specimen and crack sizes, water/cement ratio and coarse aggregate texture upon fracture toughness of concrete. *Magazine of Concrete Research* 36(129): 227-236.

RILEM TC-50 FMC 1985. Determination of the fracture energy of mortar and concrete by means of three-point bend tests on notched beams. *Materials and Structures* 18: 287-90.